The Journal of Supercritical Fluids 234 (2026) 106947

Contents lists available at ScienceDirect

The Journal of Supercritical Fluids

journal homepage: www.elsevier.com/locate/supflu

Development of a new polymeric formulation of rutin by supercritical antisolvent precipitation and evaluation of its nephroprotective capacity against cisplatin nephrotoxicity in rats

Alfredo G. Casanova [a,b,c], Lucía Rodríguez-Lucas [a], Sara Pahino-Villardón [d], Iria Nerea Giraldes-Fernández [d], Marta Prieto [a,b,c,1], Ángel Martín [d,*], Ana I. Morales [a,b,c,e,1]

[a] Toxicology Unit, Universidad de Salamanca, Salamanca 37007, Spain
[b] Institute of Biomedical Research of Salamanca (IBSAL), Salamanca 37007, Spain
[c] Group of Translational Research on Renal and Cardiovascular Diseases (TRECARD), Salamanca 37007, Spain
[d] Institute of Bioeconomy, Universidad de Valladolid, Valladolid 47011, Spain
[e] Group of Biomedical Research on Critical Care (BioCritic), Valladolid 47005, Spain

HIGHLIGHTS

- Rutin was successfully encapsulated in Eudragit polymers by SAS technique.
- Formulations were in-vitro/in-vivo tested against cancer-therapy nephrotoxicity.
- Formulations showed enhanced in-vitro dissolution profiles.
- A limited therapeutic efficiency was observed probably due to low in vivo stability.

GRAPHICAL ABSTRACT

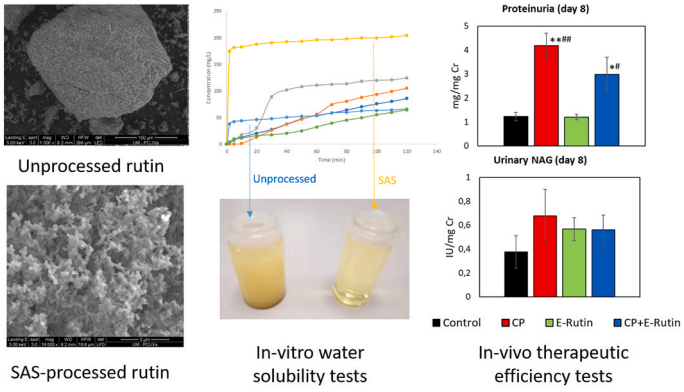

ARTICLE INFO

Keywords:
Rutin
Nephroprotection
Cisplatin
Polymeric formulation
Amorphous solid dispersion

ABSTRACT

Nephrotoxicity associated with antitumor drugs such as cisplatin is a well-documented clinical challenge. The intrinsic toxicity of these drugs is driving the search for renoprotective strategies. Currently, one of the most popular is the use of natural substances with antioxidant properties, such as flavonoids. Rutin is a member of this family whose nephroprotective properties have already been studied. However, its bioavailability is very low due to its high lipophilicity. Polymeric nanoparticle design is one of the possible strategies used to solve

Abbreviations: AKI, Acute kidney injury; AUC, Area under the concentration-time curve; Cmax, Maximum concentration in plasma; CP, Cisplatin; CrCl, Creatinine clearance; I.p., Intraperitoneal; NAG, N-Acetyl-β-D-glucosaminidase; P.o., Orally; SAS, Supercritical Anti Solvent; SEM, Scanning electron microscope.

* Corresponding author.
E-mail address: angel.martin.martinez@uva.es (Á. Martín).

[1] These authors share senior authorship.

https://doi.org/10.1016/j.supflu.2026.106947
Received 28 November 2025; Received in revised form 20 February 2026; Accepted 26 February 2026
Available online 27 February 2026

pharmacokinetic problems. The aim of this work was to design and develop a new polymeric formulation of rutin and to evaluate its nephroprotective capacity against cisplatin toxicity in an experimental rat model. Rutin was processed and coated with Eudragit® polymers using the Supercritical Anti Solvent (SAS) process. A successful micronization and coating of rutin was achieved. *In vitro* release studies of the formulations obtained demonstrated that pure SAS-processed rutin showed a higher solubility and dissolution rate that unprocessed rutin, and that rutin coated with Eudragit® polymers combined this increased solubilization with a controlled release. However, after administration of the formulation with the best *in vivo* properties obtained in rats, they did not show a significant nephroprotective capacity. The histological study confirmed the negative results obtained in the functional study. Although this formulation did not show significant nephroprotective effects *in vivo*, the study provides valuable insights into the limitations of current polymeric encapsulation strategies for rutin.

1. Introduction

Acute kidney injury (AKI) is an alteration with high morbi-mortality rates that occurs in approximately 10–20% of hospitalized patients and up to half of the patients admitted to the intensive care unit [1–3]. It is defined as the abrupt and rapid (within a few hours) drop in renal function [4] which, additionally, implies a high risk of developing chronic kidney disease [1]. One of its main causes is exposure to nephrotoxic drugs, which has been associated with one in four cases of AKI in hospitalized patients [3]. Specifically, nephrotoxicity associated with anticancer drugs is related to a higher risk of death in treated patients and an increase in hospital stay and associated economic costs. Besides, on many occasions it forces the interruption of oncological treatment [5].

Cisplatin is an effective antineoplastic agent that has been used for more than 50 years to treat various cancers. However, its toxicity, and especially its nephrotoxicity, limits its clinical application [6]. In fact, it is estimated that between 10% and 38% of patients treated with cisplatin suffer AKI [6,7], which has been related to processes such as inflammation, oxidative stress, mitochondrial and endothelial dysfunction, direct DNA damage, autophagy and apoptosis, among others [8–10]. Numerous strategies have been proposed to prevent cisplatin-induced AKI, such as patient hydration with magnesium and/or potassium supplementation [11,12] and administration of drugs (such as N-acetylcysteine [13], mannitol [14], and liraglutide [15], among others) and other compounds of natural origin, as flavonoids.

Flavoloids are phenolic or polyphenolic compounds of plant origin present in various fruits and vegetables [16] that have been postulated as suitable candidates to prevent cisplatin-induced AKI due to their antioxidant, anti-inflammatory and anti-apoptotic properties [17]. Some flavonoids that have already shown nephroprotective effects in this context are quercetin [18], 6-hydroxyflavone [19], resveratrol [20], and hesperidin [21]. Rutin (also called rutoside or quercetin-3-O-rutinoside [22]) is a member of the flavonoids family that is present in plants and fruits such as buckwheat, passion flower, tea and apple [23]. It has gastroprotective, hepatoprotective, antimicrobial, antidiabetic, anti-inflammatory and cancer cell resistance reducing properties, among others [23–28]. In addition, rutin is a glycoside of quercetin, so it could be responsible for some of the beneficial effects of quercetin [29]. Based on these properties, it has shown nephroprotection against cisplatin-induced renal damage in preclinical studies [30–32]. However, despite the benefits observed in cellular and animal models, its translation to the clinical setting is limited by its low stability and bioavailability, which are related to the low water solubility of this molecule [33]. For example, a study conducted with rats administered an approximate dose of 34.856 mg/kg of rutin reported an average maximum concentration in plasma (Cmax) of 1.546 mg/L and an average area under the concentration-time curve (AUC) of 9.947 mg·h/L [34]; and another study in humans administered 662 μMol rutin (equivalent to 200 mg quercetin) reported an average Cmax of 0.32 μg/mL and an average AUC from 0 to 24 h of 2.5 μg·h/mL [35].

A promising approach to overcome these physicochemical limitations is the inclusion of rutin and other flavonoids in nanoparticulate systems [33,36], some of which are polymeric particles that convey favorable properties for drug transport, such as the capacity to transport drugs in inclusion compounds, micellar suspensions or liposomes, among others [37]. There are several recent studies in which nanoparticle formulations containing rutin are produced and evaluated, including, for example, silver nanoparticles with antithrombotic properties [38], chitosan and alginate nanoparticles with antidiabetic potential [39], zinc oxide-coated nanoparticles with antibacterial effect [40], and hyaluronic acid nanoparticles with vasculoprotective properties [41]. Among other possible carrier polymers, Eudragit® is the trade name of a family of polymethacrylate compounds that are synthetically obtained from dimethylaminoethyl methacrylates, methacrylic acid, and methacrylic acid esters [42]. They are polymers used for the coating of pH-dependent enteric formulations in order to increase the solubility of hydrophobic compounds as well as to protect them from the acid pH of gastric juice, thus avoiding their degradation and allowing the design of pH-sensitive drug delivery systems [43].

The particle size and crystalline structure of active components such as rutin also play a role on the stability and bioavailability of these components. In general, the reduction of particle size together with the production of particles with an amorphous, non-crystalline structure, can improve the solubilization of the compound and enhance the bioavailability. Stabilization of these non-crystalline particles into a polymer such as Eudragit®, that can further contribute to solubilize the compound and protect it from acidic gastric conditions [44], can promote the bioavailability of rutin and therefore its therapeutic activity, as shown in previous results obtained from other researchers with Eudragit®-encapsulated quercetin [45].

Particle processing techniques based on the use of compressed and supercritical fluids, and in particular the Supercritical Anti Solvent (SAS) technology, offer advantages for the development of such polymer-flavonoid formulations, such as an enhanced control over particle size and morphology, the operation at mild temperature conditions and in an inert atmosphere, which prevents the degradation of sensitive compounds such as flavonoids, and the possibility to obtain solvent-free products without any additional downstream processing [46]. SAS technique is able to micronize and to co-precipitate a wide range of active compounds and carrier materials, provided that they can be solubilized in a solvent with a high solubility in supercritical CO_2, and that the solutes themselves have a low solubility in CO_2. For co-precipitation applications, the process is made easier if the solute and the carrier material can be solubilized in the same solvent; in the current study, that is the case with ethanol, that can solubilize both rutin and the Eudragit® polymers used for coating the active compound. Previous studies have already demonstrated the possibility to encapsulate active compounds in Eudragit® polymers [47], including as application examples the coating of curcumin [48] or propolis extracts [49]. Similarly, previous studies have demonstrated the SAS micronization of rutin [50].

Based on this background and on favorable results obtained by our research group with other flavonoids included in polymeric systems, such as the Pluronic® F127-quercetin (P-quercetin) formulation presented in a previous work [51], the aim of this work is to develop a new polymeric formulation based on Eudragit® containing rutin and to evaluate its ability to protect against cisplatin-induced AKI in rats.

2. Materials and methods

All chemicals and reagents were purchased from Merck (Darmstad, Germany) except where otherwise indicated.

2.1. Preparation of the polymeric formulation of rutin

Rutin was precipitated and coated with Eudragit® polymers via the SAS process. A detailed description of the SAS process employed has been presented in previous works [52,53]. Briefly, rutin hydrate (>94%) was purchased from Merck, while Eudragit® E-100 (cationic copolymer based on dimethylaminoethyl methacrylate, butyl methacrylate, and methyl methacrylate with a ratio of 2:1:1, average molecular weight 47,000 g/mol) and Eudragit® L-100 [Poly(methacrylic acid-co-methyl methacrylate, average molecular weight 125,000 g/mol), with a ratio of 1:1] were kindly provided by Evonik (Essen, Germany). Technical grade CO_2 (purity ≥ 97.0 vol%) was purchased from Linde (Valencia, Spain) and dehydrated ethanol (> 99.9%) was purchased from Dávila Villalobos (Valladolid, Spain).

Solutions of rutin and the Eudragit® polymers in ethanol were prepared by dissolving 1 g of rutin in 300 mL of ethanol and adding Eudragit®:rutin mass ratios of 0 g:g, 1 g:g or 2 g:g. This solution was processed with the SAS crystallization apparatus schematically shown in Fig. 1. The organic solution was pumped at a constant flow rate of 5 mL/min with a HPLC pump, while CO_2 was pumped at a flow rate of 2 kg/h with a membrane pump (Milton Roy, Pennsylvania, USA). These two streams were introduced into the precipitator (inner volume: 1.5 L) via a coaxial nozzle, whose inner diameter, for injection of the solution, was 100 μm and other diameter, for injection of CO_2, was 1.5 mm. Conditions in the precipitator were kept constant at 40 °C and 100 bar using a heating jacket and a back-pressure valve, respectively- These operating conditions were chosen based on previous results of the research group dealing with the SAS precipitation of Eudragit® polymers [48] and a similar flavonoid, quercetin [52], which indicated that these were suitable pressure and temperature conditions, and that variation of these parameters had a comparatively minor influence over product characteristics than the polymer:active component ratio. Temperature in the precipitator was measured with a Pt-100 thermoresistance, pressure was measured with a DESIN TPR-10 transducer, and CO_2 flowrate was measured with a MICRO Motion (Boulder, Colorado, USA) Elite RFT9739 Coriolis instrument.

Upon mixing of the organic solution and CO_2 in the coaxial nozzle, the solutes (rutin and polymer) precipitated by the simultaneous effect of the extraction of ethanol by supercritical CO_2 and the saturation of the ethanol with CO_2, which reduces solutes solubility by an antisolvent effect [54]. Particles thus formed were retained inside the precipitator by a 0.2 μm HPLC filter supported over a metallic frit located at the bottom of the precipitator. An additional Classic filters model SL 127.401 was placed after the precipitation vessel. In each precipitation experiment, approximately 1 g of powder was collected in experiments with pure rutin and 2 g in experiments of co-precipitation of rutin with a polymer. The effluent of the precipitator was decompressed in the back-pressure valve and its liquid and gaseous fractions were separated in the flash separation vessel.

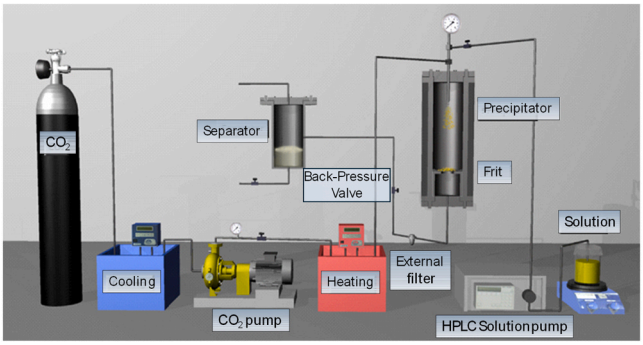

Fig. 1. Schematic representation of supercritical anti solvent plant.

2.2. Physico-chemical characterization of the formulation

Scanning Electron Microscopy (SEM) micrographs of the particles were acquired using a QUANTA 200 FEG scanning electron microscope (Thermo Fisher, Waltham, Massachusetts, USA) at magnifications of 1000 × , 4000 × , and 16,000 × . Prior to image acquisition, the samples were coated with a thin layer of gold using a sputter coater. The crystalline structure of the particles was analyzed by powder X-ray diffraction (PXRD) using a Bruker (Billerica, Massachusetts, USA) D8 Discover diffractometer equipped with a copper ceramic X-ray tube (Cu Kα radiation) operated at 2.2 kW and a 3 kW generator, in the 2θ range 5° - 65°. Solid samples were also characterized by FT-IR spectroscopy using a Bruker Alpha spectrometer equipped with a platinum ATR sampling module. Spectra were recorded in the 4000–400 cm^{-1} range at a resolution of 4 cm^{-1} , averaging 32 scans per sample.

The proportion of rutin in the rutin:Eudragit® composites was determined by UV-Vis spectrophotometry using a Shimadzu (Kyoto, Japan) UV-2550 instrument. To do so, a weighed amount of the SAS-produced formulation was redissolved in ethanol and loaded in a quartz cell (optical length: 1 cm). The concentration of rutin in this solution was derived from its absorbance at 418 nm based on a calibration line set measuring the absorbance of solutions of rutin + Eudragit® polymers in ethanol of known compositions in the range 0 – 3.5 mg/L. The preparation and measurement of the standards for the calibration line and the measurement of rutin in SAS formulations was carried out in triplicate.

2.3. In vitro solubility/release study

In vitro solubility tests in simulated intestinal fluids were performed using a Coplay Scentific Ltd. (Nottingham, UK) dissolution test apparatus operated in the basket mode. Simulated intestinal fluids were chosen as the model fluid for dissolution tests because it is expected that rutin is mainly absorbed by the organism in the intestine. The apparatus employed is a certified apparatus for *in vitro* dissolution tests according to Ph. Eur., USP and associated Pharmacopoeias.

To do so, simulated intestinal fluid was prepared dissolving 6.8 g of monobasic potassium phosphate (99.5%) in 1 L of ultrapure water and adjusting pH = 6.8 by dropwise addition of an aqueous 1 mol/L solution of NaOH. Each vessel of the dissolution test apparatus was filled with 475 mL of this solution. The rutin formulations were put inside clean filter bags made of cellulose and introduced in the baskets of the dissolution test apparatus. The solutions were thermostated at 37 °C and agitation was set at 100 rpm. Samples (3 mL) were collected at predefined intervals (2–120 min), and an equal volume of fresh simulated intestinal fluid was added to maintain consistency. These samples were filtered using a syringe filter (pore size: 0.2 μm) and then analyzed by UV–visible spectrophotometry as described in the previous section to determine the concentration of rutin.

2.4. Experimental animal model

All procedures were approved by the Bioethics Committee of the University of Salamanca and the Regional Government of Castile and Leon, Ministry of Agriculture and Livestock (reference: 787; 27 July 2022). Animals were handled according to the guidelines of the Directive 2010/63/EU of the European Parliament and of the Council and to the current Spanish legislation for experimental animal use and care. The animals were maintained throughout the study under stable and controlled environmental conditions and with unlimited access to water and food.

A nephrotoxicity model consisting of the administration of a single dose of cisplatin (5 mg/kg) intraperitoneally (i.p.) was used [55–57]. Sixteen healthy male Wistar rats weighing between 200 and 220 g from the Animal Experimentation Service of the University of Salamanca were randomly distributed seeking homogeneity of weights in the following groups (n = 4) (Fig. 2): Control, that received a daily dose of 0.1 g/mL sucrose and 2 μL/mL vanilla extract (these two components improve organoleptic properties and, therefore, acceptance in rats of daily administration of the formulation) in drinking water (rutin formulation vehicle) orally (p.o.) for 12 days, and an i.p. dose of NaCl 0.9% (cisplatin vehicle) on day 6 of the experiment; CP, that received a daily dose of vehicle p.o. for 12 days, and an i.p. nephrotoxic dose of 5 mg/kg of cisplatin on day 6; E-Rutin, that received a daily dose of 200 mg/kg of the SAS-processed rutin + Eudragit® L100 coprecipitate (hereafter, E-Rutin), containing 100 mg/kg rutin, p.o. for 12 days, and an i.p. dose of NaCl 0.9% on day 6; and CP+E-Rutin, that received a daily dose of 200 mg/kg of E-Rutin p.o. for 12 days, and an i.p. dose of 5 mg/kg of cisplatin on day 6. The dose of E-Rutin (200 mg/kg, equivalent to 100 mg/kg of rutin) was selected based on similar studies performed with this flavonoid (doses between 30 and 200 mg/kg showed nephroprotective effects [30,31,58–62]) and considering the characteristics (mainly the ability to be administered) of the suspension resulting from the incorporation of the formulation in the administration vehicle. A total of approximately 10 g of E-Rutin was consumed in these experiments; this amount was produced in 5 independent SAS precipitation experiments. The powder produced in these experiments was mixed and homogenized before beginning the study.

The animals were weighed every day, and blood and urine samples were collected on days 0, 6, 8, 10 and 12 of the experiment. For the collection of urine excreted for one day, metabolic cages were used, in which the rats were introduced 24 h prior to the days indicated above. The urine samples were subsequently centrifuged at 2000 × g for 9 min (to remove possible solid particles) and stored at −80 °C. On the other hand, blood samples were extracted with heparinized capillaries after making a small incision in the animal's tail. They were then centrifuged at 11,000 rpm (20,000 g) for 3 min and the resulting plasma was stored at −80 °C. On day 12 (the final day of the experiment), the animals were euthanized. For this purpose, the rats were anesthetized and exsanguinated, after which their kidneys were removed and fixed in 3.7% paraformaldehyde for histological studies.

2.5. Evaluation of renal function

Creatinine was measured in plasma and urine samples using a commercial kit based on the Jaffe method [63] ("QuantiChrom Creatinine Assay Kit", BioAssay Systems, USA). CrCl was calculated from weight and plasma creatinine with "ACLARA", an online calculator developed by our research group [64]. Proteinuria was measured using the Bradford method [65], and urinary NAG activity was quantified using a commercial kit ["N-Acetyl-β-D-glucosaminidase (NAG) assay kit", Diazyme, USA].

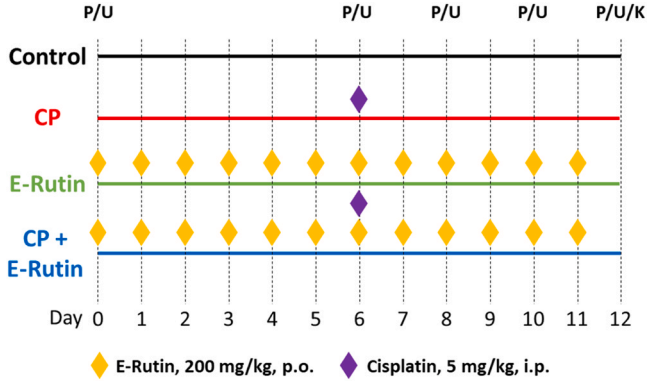

Fig. 2. Experimental protocol. CP, cisplatin; i.p., intraperitoneal; K, kidneys collection; P, plasma collection; p.o., per os (oral route); U, urine collection.

2.6. Histopathological study

Para-formaldehyde fixed kidneys were embedded in paraffin and 5 μm tissue sections were stained with hematoxylin and eosin. Damage quantification was performed in a blind manner as follows: fifteen representative random photographs of the complete kidney (five of the cortex, five of the corticomedullary region and five of the medulla) were taken for each animal. Each image was divided into 6 quadrants of the same size, to which a lesion score was attributed according to the following criteria: presence of apoptosis (+1) or necrosis (+2), few/small (+1) or many/large (+2) vacuoles, and tubular dilatation (+1) with proteinaceous deposits (+1). Photographs were taken under an Olympus BX51 microscope connected to an Olympus DP70 color, digital camera (Olympus, Madrid, Spain).

2.7. Statistical analysis

The normality of the data was tested with the Saphiro-Wilk test. Subsequently, comparison of quantitative variables between groups was performed with the parametric ANOVA test coupled with the Scheffe test (for normal variables) or the nonparametric Kruskal-Wallis test coupled with the Bonferroni correction as post-hoc analysis (for non-normal variables). p-values < 0.05 were considered statistically significant. The analysis described above was carried out with IBM SPSS Statistics 28 (International Business Machines®, Armonk, NY, USA).

3. Results

3.1. Supercritical Anti Solvent (SAS) coprecipitation of rutin and Eudragit® polymers: physico-chemical characterization of the formulations

Fig. 3 shows a comparison of scanning electron micrographs of unprocessed rutin and SAS-micronized rutin. For ease of comparison, both images are presented with the same magnification ratio.

As it can be seen in Fig. 3a, the untreated rutin showed irregularly shaped particle aggregates with sizes between 80 and 200 μm. In Fig. 3b, when the rutin was processed with the SAS method, the particles had a very porous, sponge-like surface and smaller particle size, in agreement with results reported by Montes et al. [50]. As observed in the SEM microscopy, aggregates of 10 – 50 μm made of nanoparticles of less than 100 nm were obtained.

Fig. 4 presents the X-ray diffraction diagrams of the commercial rutin and the SAS-processed rutin. The diffractogram of the commercial rutin shows intense peaks at $2\theta = 5.17°$, 7.28°, 10.53°, 14.84°, 16.69°, and 26.73°, indicating that it has a crystalline structure [50,66]. However, the rutin processed with SAS showed a flat diffractogram, without characteristic peaks, indicating that it is an amorphous material, which can enhance the solubility and bioavailability of the compound.

FT-IR spectra of commercial and SAS-processed rutin are presented in Fig. 5. The main characteristic bands in the FT-IR spectrum of the commercial rutin correspond to the stretch of the carbonyl group at 1654–1600 cm^{-1} and that of the ether group at 1362–1169 cm^{-1} [67,68]. The prominent band at 3406 cm^{-1} corresponds to the stretching of the hydroxyl group, while the band at 2958 cm^{-1} is due to the C–H bond [67] and a last prominent band at 1383 cm^{-1} corresponds to the vibrations of the C–OH bond [69].

The FT-IR spectra of commercial and SAS-processed rutin show significant differences. First, in the SAS-processed rutin, the stretch band of the hydroxyl group, located between 3500 and 3000 cm^{-1} shows a greater concavity, which is consistent with the dehydration of the material due to SAS precipitation. Moreover, a band appears with greater

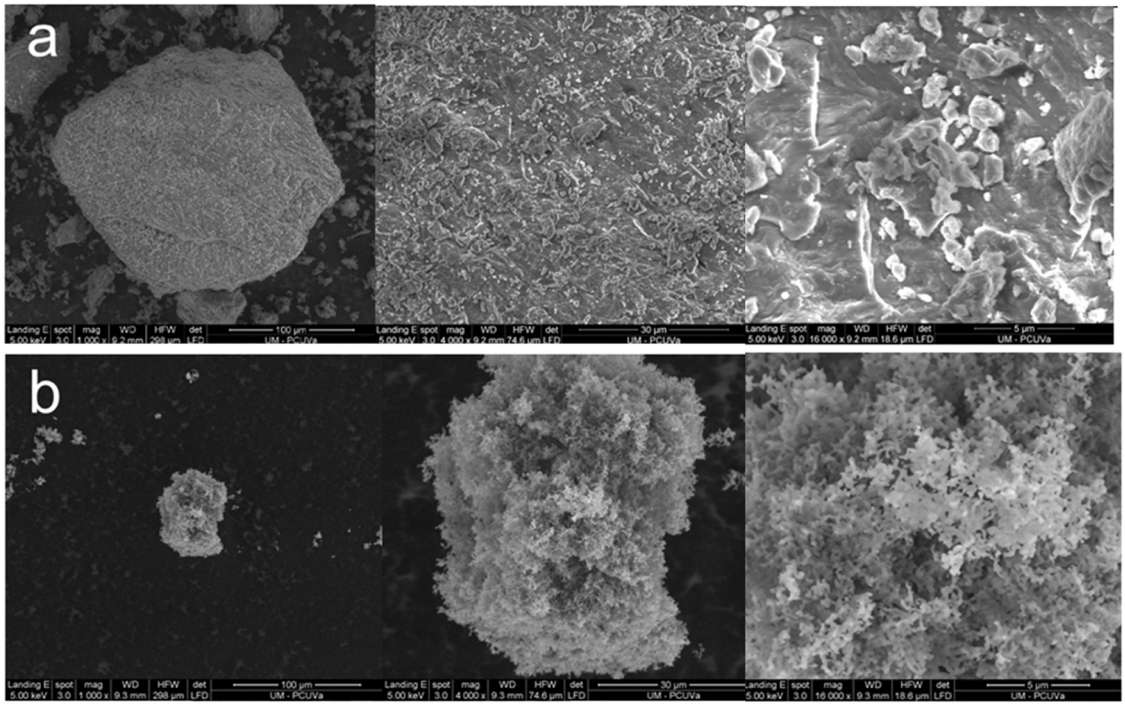

Fig. 3. Scanning electron microscope micrographs of (a) commercial and (b) SAS-processed rutin. The images are presented with the same magnification ratio: 1000x on the left, 4000x on the center, and 16000x in the right, corresponding to a scale of 100 μm, 30 μm, and 5 μm, respectively.

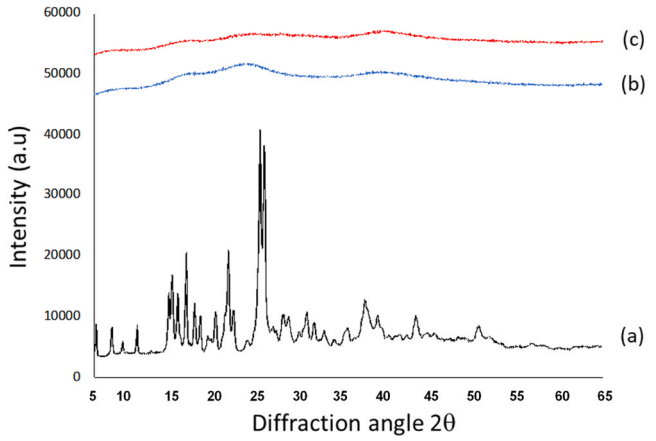

Fig. 4. X-ray diffractogram (a) commercial rutin, (b) SAS-precipitated rutin, (c) SAS-precipitated rutin (repeated experiment). For clarity, diffractograms are vertically displaced by arbitrary amounts. a.u, arbitrary units.

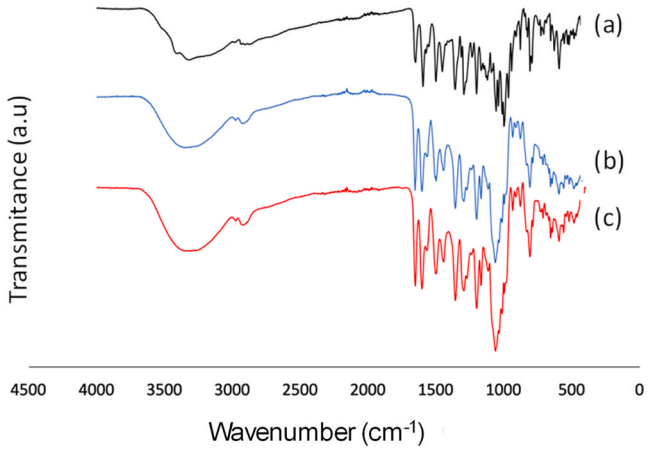

Fig. 5. FT-IR spectra (a) commercial rutin, (b) SAS-processed rutin, (c) SAS-processed rutin (repeated experiment). For clarity, diffractograms are vertically displaced by arbitrary amounts. a.u, arbitrary units.

intensity at 1654–1600 cm^{-1} which, as indicated above, corresponds to the stretching of the carbonyl group. Another important difference is the band between 1362–1169 cm^{-1}, corresponding to the ether group, which is appreciably wider in the processed samples. All these differences in spectra can be linked to variations in the structure of the material due to the formation of anhydrous rutin [52].

In the case of rutin-Eudragit® coprecipitation experiments, constant pressure, temperature, and flow rate conditions of 100 bar, 40 °C, 5 mL/min of organic solution and 2 kg/h of CO_2 were applied, as previously described. Different concentrations of Eudragit® in the organic solution, corresponding to different polymer:rutin ratios, were tested. This ratio was chosen as a main process parameter to be tested, because previous results on the coating and encapsulation of active compounds by coprecipitation with polymers using the SAS technique indicated that this ratio is the main parameter influencing the morphology and properties of the particles formed [52].

In particular, two polymer:rutin ratios, 1:1 g and 2:1 g were tested in experiments reported in this work. With the second ratio of 2:1 g, it was observed that SAS experiments did not yield particles, but a film instead that covered the filter and most of the inner surface of the precipitator, which could not be recovered for characterization and was not a suitable morphology of the product for its application. Experiments with a 1:1 g mass ratio, in contrast, successfully yielded a finely micronized product. Fig. 6 shows SEM micrographs of this product obtained with the 1:1 g mass ratio.

The morphologies obtained indicate that the rutin particles act as crystallization nuclei and are covered by a polymer film that also restricts the growth of the rutin particles. Compared with the morphology of SAS-processed pure rutin (Fig. 3), aggregates of comparable sizes of 10 – 50 μm are obtained, but with the constituting individual

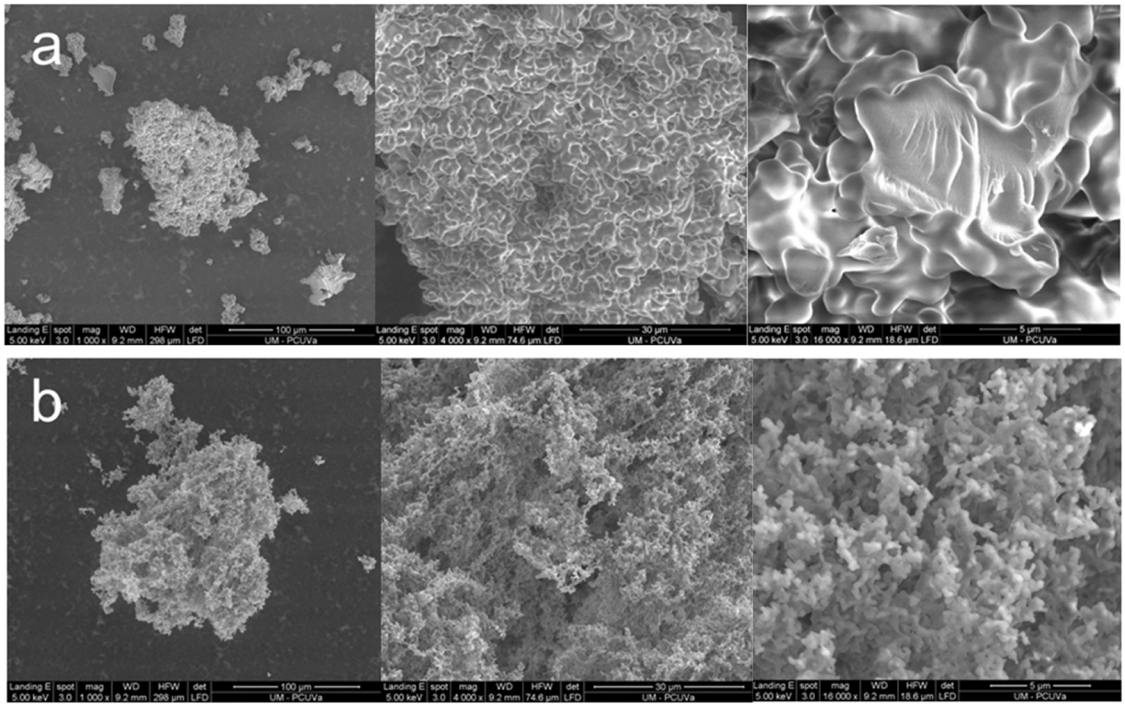

Fig. 6. Scanning electron microscope micrographs of particles obtained by SAS coprecipitation of rutin and Eudragit®: (a) rutin/Eudragit® E100, polymer/rutin ratio 1 g/1 g and (b) rutin/Eudragit® L100, polymer/rutin ratio 1 g/1 g. The images are presented with the same magnification ratio: 1000x on the left, 4000x on the center, and 16000x in the rightru, corresponding to a scale of 100 μm, 30 μm, and 5 μm, respectively.

nanoparticles of rutin coated by a polymer film, which is particularly apparent in samples co-precipitated with Eudragit® E100 (Fig. 6a). Compared with this, the polymer film is less apparent in samples coprecipitated with Eudragit® L100 (Fig. 6b). This result is consistent with the tendency of Eudragit® E100 to form lumps at mild temperatures above 30 °C as stated by manufacturers [70], a behaviour that is not presented by Eudragit® L100. Nevertheless, in both cases, it can be clearly seen how the polymer is introduced between the interstices of the particles, completely covering them, indicating that the polymer concentration is high enough for a complete coating of the active compound [52].

To verify that the composition of these particles corresponds to the concentration of the initial organic solution fed to the SAS process, particle composition was analyzed by UV–vis spectrophotometry. As shown in Table 1, the concentration of particles indeed corresponded to the 1:1 mass ratio in the initial organic solution, showing that the powder produced by SAS precipitation retained the composition of the initial solution.

The structural properties of Eudragit®-coated rutin were studied by X-ray diffraction. The results are shown in Fig. 7. The pure Eudragit® diagrams (Figs. 7b and 7c) correspond to those reported in the literature [71,72]. As expected, the diffractogram of a physical mixture of rutin and raw Eudragit® just showed the superposition of the diagrams of both pure compounds (Figs. 7f and 7g).

Table 1
Theoretical and experimental composition of rutin/Eudragit® coprecipitates. Data are presented as mean ± standard deviation, based on three replications of the analysis.

Sample	Theoretical composition (% mass rutin)	Experimental composition (% mass rutin)
Rutin/Eudragit® E100	50	49.6 ± 0.6
Rutin/Eudragit® L100	50	48.3 ± 0.6

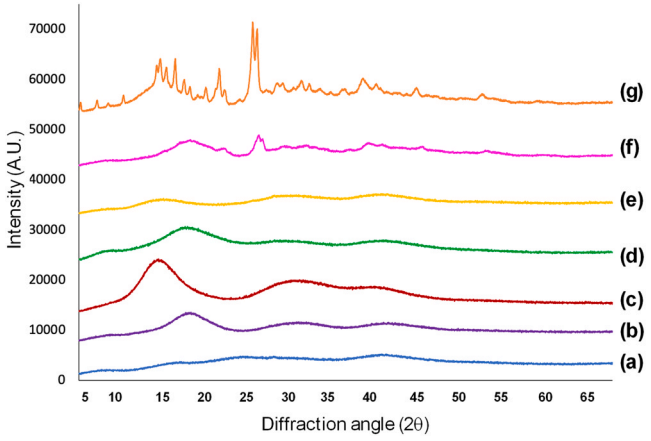

Fig. 7. X-ray diffractograms (a) SAS-processed rutin, (b) Eudragit® E100, (c) Eudragit® L100, (d) SAS coprecipitated rutin and Eudragit® E100, (e) SAS coprecipitated rutin and Eudragit® L100, (f) rutin + Eudragit® E100 physical mixture without SAS processing (g) rutin + Eudragit® L100 physical mixture without SAS processing. For clarity, all diagrams have been vertically displaced by arbitrary amounts. a.u, arbitrary units.

The X-ray diffraction pattern of rutin shows sharp peaks indicating that this flavonoid is crystalline in nature, while the pattern of Eudragit® shows blunt peaks indicating its amorphous nature. When samples are subjected to the SAS process, the rutin forms a solid dispersion with the Eudragit® and the sharp peaks of the rutin are attenuated (Fig. 7d and e), demonstrating that coprecipitation experiments resulted in products with an amorphous structure [52].

As discussed in previous sections, co-precipitation techniques using polymers can be used to produce inclusion complexes or micellar structures, which can improve the solubility and dissolution rate in water. The possible interactions between the polymer and the active compound can be characterized by FT-IR spectroscopy [73,74]

Fig. 8 presents the FT-IR spectra of rutin samples co-precipitated with Eudragit®. The spectra of polymeric materials (Fig. 8b and c) show characteristic bands of esterified groups at 1150–1190, 1240 and 1270 cm^{-1}, as well as the vibration of the carbonyl group at 1730 cm^{-1}. In addition, vibrations were observed in the hydrocarbon chain at 1385, 1450–1490, and 2950 cm^{-1} [75]. On the other hand, the spectra of the rutin co-precipitated with Eudragit® by the SAS process, as well as the spectra of pure rutin, show an attenuation of the hydroxyl group band due to dehydration of the compound and additional peaks were observed at 1730 cm^{-1} corresponding to the Eudragit® carbonyl group and at 1150–1190 cm^{-1} of the ester groups, as mentioned above. Apart from this, no additional peaks or shifts in the characteristic bands were observed, indicating that no chemical interactions or complexes occurred between the carrier and the rutin [52,75]. Therefore, and as already indicated by SEM-micrographs, it can be concluded that the formulations are constituted by rutin micro and nanoparticles coated by a polymer film.

3.2. In vitro dissolution tests

Fig. 9 shows the results of the *in vitro* dissolution tests. The most remarkable result in terms of the increase of the dissolution rate was obtained with SAS-processed pure rutin, which showed a much faster dissolution rate as well as a higher final solubility than the commercial rutin. This feature was also obvious by a simple visual inspection of the dissolution process: while addition of unprocessed rutin to water resulted in a turbid suspension, indicating that rutin was not dissolved, addition of SAS-processed rutin to water nearly immediately produced a transparent, yellow-colored solution, indicating a successful dissolution of the compound. This result can be attributed to the change in the particle size and crystalline structure of particles which, as previously indicated, in SAS experiments corresponded to sub-micrometric, amorphous particles, compared to the larger and highly crystalline particles constituting the commercial rutin. Both features can promote the dissolution rate as well as the solubility of the material.

On the other hand, it can be observed that a physical mixture of rutin with either Eudragit® L-100 or Eudragit® E-100 promotes solubility with respect to the pure commercial rutin. In the case of Rutin + E100, the physical mixture shows a slow initial release, followed by a burst release after about 20 min. A similar result was reported by Mathur et al. [76], who showed increases in the dissolution rate of rutin encapsulated in Eudragit® polymers, especially at simulated intestinal pH conditions. Asfour and Mohsen [77] reported similar dissolution curves for Eudragit®-encapsulated rutin, in this case prepared by a liquid anti-solvent method, with enhanced release at simulated intestinal conditions. SAS-processed coprecipitates show a faster dissolution rate than physical mixtures at short times, but much slower dissolution rates and lower final solubilities than the pure SAS-processed rutin. This indicates that the polymer coating regulates the dissolution rate of the material, which may be more favorable for *in vivo* applications than the burst-dissolving SAS-processed rutin. Based on this result, the SAS-coprecipitated rutin + Eudragit® L-100 (E-rutin), that provides a high initial dissolution rate together with a sustained continuous release along longer dissolution times, was selected for further *in vivo* evaluation tests.

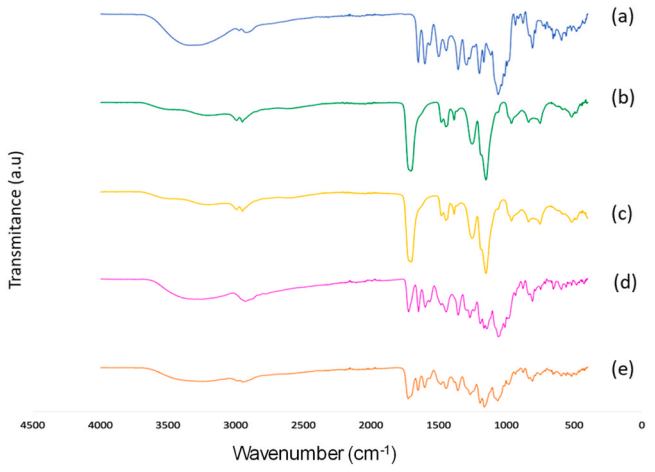

Fig. 8. FT-IR spectra (a) SAS-processed rutin, (b) Eudragit® E100, (c) Eudragit® L100, (d) SAS coprecipitated rutin and Eudragit® E100, (e) SAS coprecipitated rutin and Eudragit® L100. For clarity, all diagrams have been vertically displaced by arbitrary amounts. a.u, arbitrary units.

3.3. In vivo evaluation: body weight and renal function

During the entire period of E-Rutin administration prior to AKI (days 0–6) all rats showed stable body weight (indirectly indicating the safety of the polymeric formulation; $p > 0.05$ versus Control). From day 6, however, the groups receiving the nephrotoxic dose of cisplatin showed a decrease in body weight, which was statistically significant from day 10 for both groups ($p = 0.028$ for the CP group; and $p = 0.020$ for the CP+E-Rutin group versus Control) and was not ameliorated by E-Rutin (Fig. 10a).

Regarding renal function (Fig. 10b), rats in the CP group (except for one of them, which showed no evident nephrotoxicity, so its data were eliminated from the entire study) underwent AKI evidenced by a maximum peak in their plasma creatinine and a minimum value in their creatinine clearance (CrCl) on day 10 (4 days after cisplatin administration). Rats in the CP+E-Rutin group also underwent AKI with the same time profile, although their plasma creatinine levels were lower (although not at a statistically significant level, $p > 0.05$) than those in the CP group. As for their CrCl, it showed the same evolution as the group that only received cisplatin ($p > 0.05$). On the other hand, the Control and E-Rutin groups showed no changes in these biomarkers throughout the experiment.

The urinary biomarkers of renal damage evaluated, proteinuria and N-Acetyl-β-D-glucosaminidase (NAG), showed peak excretion in the CP group at day 8 (Fig. 11). The levels of urinary excretion of total protein in this group increased significantly with respect to the groups without renal damage ($p = 0.002$ versus Control; and $p = 0.002$ versus E-Rutin). The CP+E-Rutin group also had an increase in protein excretion ($p = 0.037$ versus Control; and $p = 0.034$ versus E-Rutin), which was slightly lower than that of the group with maximal nephrotoxicity ($p > 0.05$ versus CP). NAG levels did not increase significantly in any of the study groups ($p > 0.05$ among all groups), although the CP group showed the highest mean value.

3.4. In vivo evaluation: histopathological study

Representative images of the renal cortex and medulla in each study group are shown in Fig. 12a and b, respectively. No structural damage was observed in the Control and E-Rutin groups. However, both the CP and CP+E-Rutin groups showed generalized renal lesions, including the presence of tubular dilatations without/with proteinaceous deposits, apoptosis and cellular necrosis and vacuolization, with the medullary region being more affected. The quantification of the damage is shown in Fig. 13. No improvement was observed in the CP+E-Rutin group with respect to the CP group, neither at cortical nor medullary level nor when the whole renal structure is considered ($p > 0.05$ between these two groups in the three quantifications).

4. Discussion

In this research work, a new rutin formulation has been designed and generated which, in spite of improving some of its physicochemical properties, does not show nephroprotective effects in the experimental

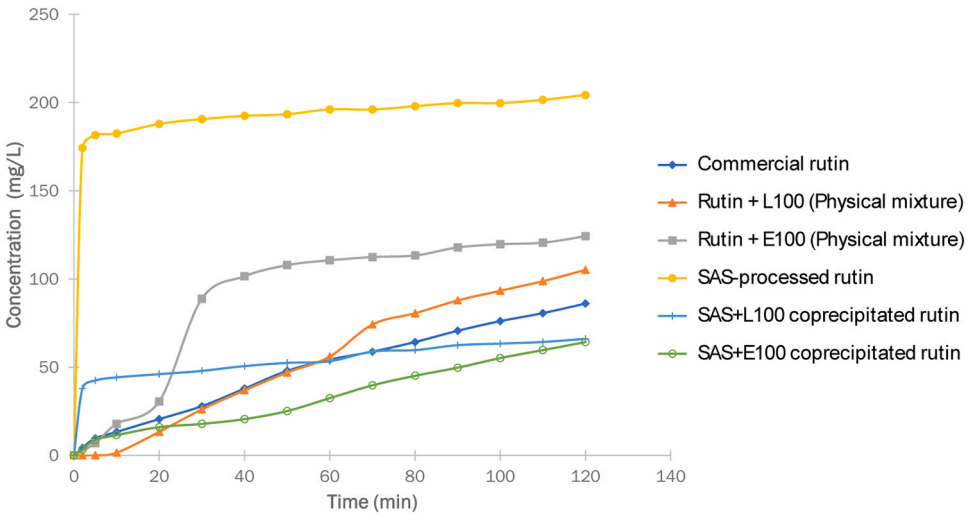

Fig. 9. *In vitro* dissolution curves in simulated intestinal fluids. SAS, Supercritical Anti Solvent.

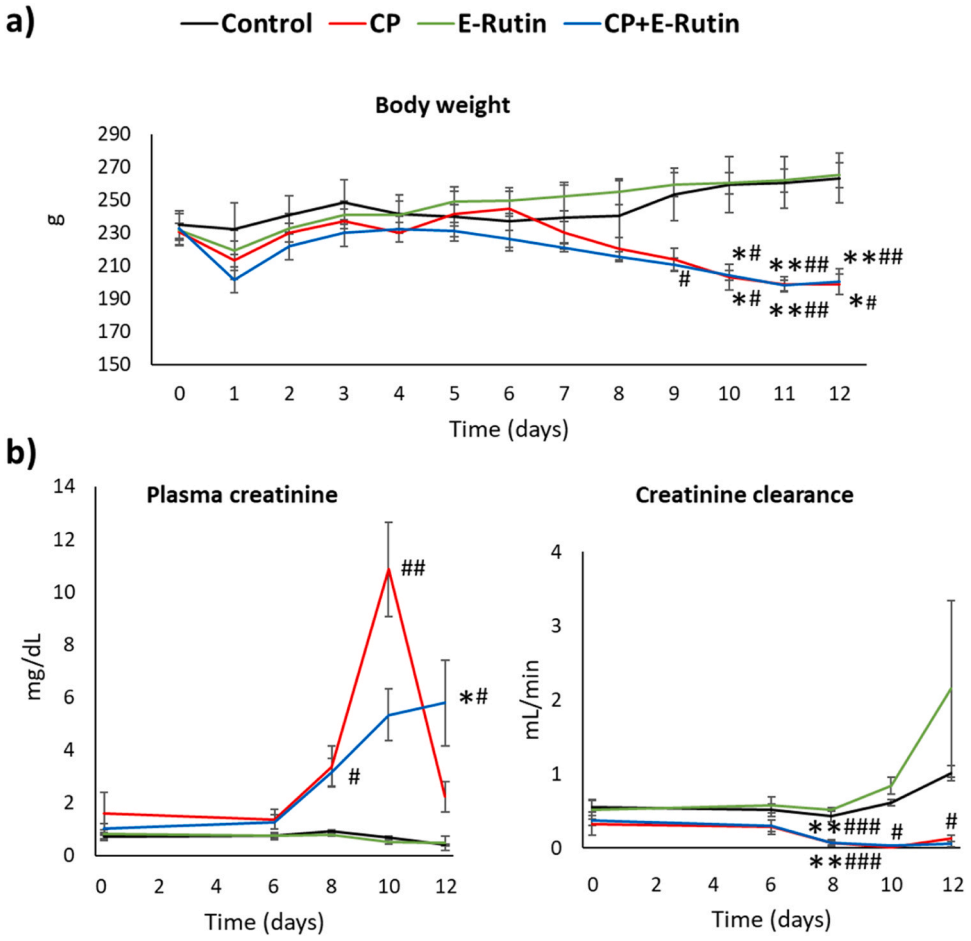

Fig. 10. Evolution of body weight (a) and plasma creatinine and creatinine clearance (b) over time (n = 4 for all groups except for the CP group, with n = 3). Data are presented as mean ± standard error of the mean. * $p < 0.05$; ** $p < 0.01$ versus Control group; # $p < 0.05$; ## $p < 0.01$; ### $p < 0.001$ versus E-Rutin group. CP, cisplatin.

model used.

The development of new formulations that improve the pharmacokinetic properties of flavonoids and facilitate their implementation in the clinical setting is a recurrent strategy at present [78–80]. In our study, two polymeric systems were formulated that included rutin as the active principle. Among them, the formulation SAS-encapsulated rutin in Eudragit® L100 (E-Rutin) was selected because it presented a solubility profile that is faster in the early stages but more sustained and controlled as time progresses, and therefore an interesting compromise between the very fast, burst dissolution achieved with the SAS-processed

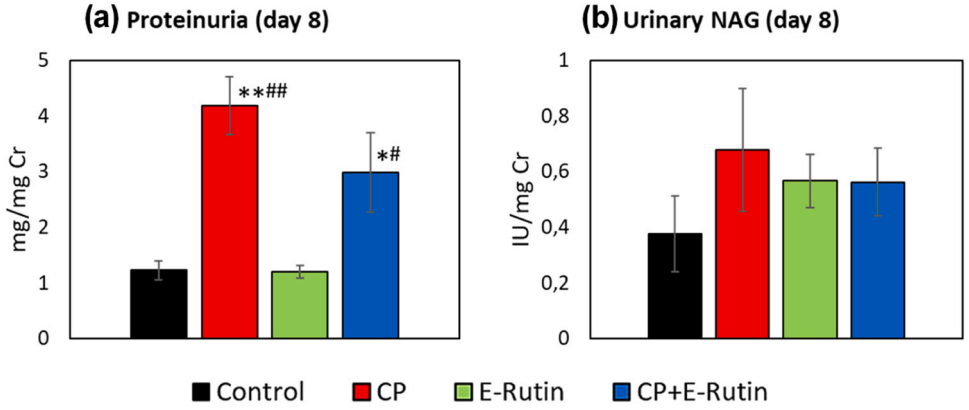

Fig. 11. Urinary protein (a) and NAG excretion (b) on day 8 of the experiment (n = 4 for all groups except for the CP group, with n = 3). Data are presented as mean ± standard error of the mean. * $p < 0.05$; ** $p < 0.01$ versus Control group; # $p < 0.05$; ## $p < 0.01$ versus E-Rutin group. CP, cisplatin; Cr, creatinine; NAG, N-acetyl-β-D-glucosaminidase.

pure rutin, and the slow release provided by rutin + Eudragit® E100 coprecipitates. However, in some cases, formulations that show favorable physicochemical properties in *in vitro* studies are not able to exert *in vivo* effects (which is usually related to the inclusion of variables that are not present in *in vitro* studies). In our case, when evaluating the nephroprotective capacity of the formulation *in vivo* by the oral route the results obtained suggest the absence of a significant nephroprotective effect attributable to the rutin-Eudragit® L100 formulation tested. This has been verified after analyzing a series of biomarkers commonly used today to diagnose kidney damage (plasma creatinine, creatinine clearance, proteinuria and NAG) [81]; and after performing a semi-quantitative evaluation of histological damage. The only parameters that show a tendency to improve in cisplatin-treated animals when the polymeric formulation is administered are plasma creatinine and proteinuria. Increased plasma creatinine is one of the signs associated with cisplatin nephrotoxicity [82], and in particular it peaks approximately four days after single administration in rats [83,84]. In our model, E-Rutin was able to dampen the elevation of this biomarker on day 4, but did so non-significantly. Moreover, this effect was not maintained on day 6 (at which time the rats begin to recover their renal function). Proteinuria, which showed its peak elevation two days after cisplatin administration, was minimally reversed by the polymeric formulation. Both findings do not allow us to state that E-Rutin exhibited nephroprotective effects.

Rutin is one of the most predominant glycosylated forms of quercetin [85]. When administered orally, it is chemically stable in the stomach [29] and is absorbed in the small intestine. However, this absorption is slower than that of quercetin (reaching its maximum plasma concentration within 7–10 h) [86]. The selected E-rutin formulation had release properties that in principle could adapt to these characteristics, i.e. an initial fast release of a certain amount of quercetin in the stomach that could be available for absorption in the small intestine together with a more sustained release at longer times, but in view of our results, it appears that effective blood concentrations are not reached. Although E-Rutin showed improved solubility *in vitro*, limited gastrointestinal stability, metabolism, and absorption likely prevented effective plasma levels, which could justify the lack of nephroprotective effects observed in the animal model. Possible explanations for the lack of efficacy of E-rutin could be degradation of the formulation *in vivo*, ineffective absorption or its limitations for the release of the active substance. Although specific stability studies in simulated gastric or intestinal fluids were not performed, the physicochemical characterization (FT-IR, XRD, and dissolution tests) and the known pH-dependent properties of Eudragit® L100 provide indirect evidence suggesting partial protection against acidic degradation and controlled release at intestinal pH [87–89]. Still, partial degradation or premature dissolution cannot be ruled out, and future studies should include stability and degradation assays under simulated digestive conditions to confirm these hypotheses. Furthermore, pharmacokinetic studies should also be carried out in order to determine the plasma concentration of rutin and its derivatives and therefore to assess if the active compound has reached the bioavailability levels required for a significant therapeutic efficiency. These assays, that were not performed in the current work, would allow demonstrating if the lack of therapeutic efficiency was due to a poor absorption of rutin.

On the other hand, we do not consider that the ineffectiveness of the formulation is related to an under-dosage of rutin, since the selected dose (100 mg/kg/day) and even lower doses have been found to be effective in other similar studies by other authors [30,58,90]. It is concluded, therefore, that the properties provided by Eudragit® L100 are not suitable for encapsulating this flavonoid, despite the fact that it has been used to encapsulate other active ingredients, such as tenofovir [87], enoxaparin [88], and even to formulate vaccines [89].

Another possible reason that may justify the failure to find significant protection is the high renal toxicity achieved with this nephrotoxicant. In this case, although the formulation would have achieved a favorable absorption profile and effective rutin blood levels, these would have been unable to prevent the damage caused by the antineoplastic. In other studies performed with cisplatin [30,58], even at higher doses [31,91], the maximum plasma creatinine concentration was considerably lower than that obtained in this study. This result can likely be attributed to differences in experimental conditions, including rat strain, age, baseline renal function, and cisplatin administration protocol (dose, route, and frequency). Inter-laboratory variations in animal handling, housing conditions, and analytical methods may also contribute. The histological damage observed in the tissue is also very noticeable, so that the toxicity of cisplatin is still very evident also at the structural level. Both these morphological and functional findings are consistent with each other since the presence of structural damage is manifested by worse renal function. For these reasons, our future proposal is to test whether the formulation could be effective against less renally toxic drugs such as, for example, aminoglycosides [92]. Another possible approach would be to evaluate the nephroprotective capacity of rutin nanoparticle formulations based on other polymers.

5. Conclusions

Rutin was successfully co-precipitated with Eudragit ® polymers with the Supercritical Anti Solvent (SAS) process, yielding Amorphous Solid Dispersions in which the reduction of the particle size, the production of amorphous particles and the polymer coating yielded significant improvements in the *in-vitro* dissolution profiles of the powder.

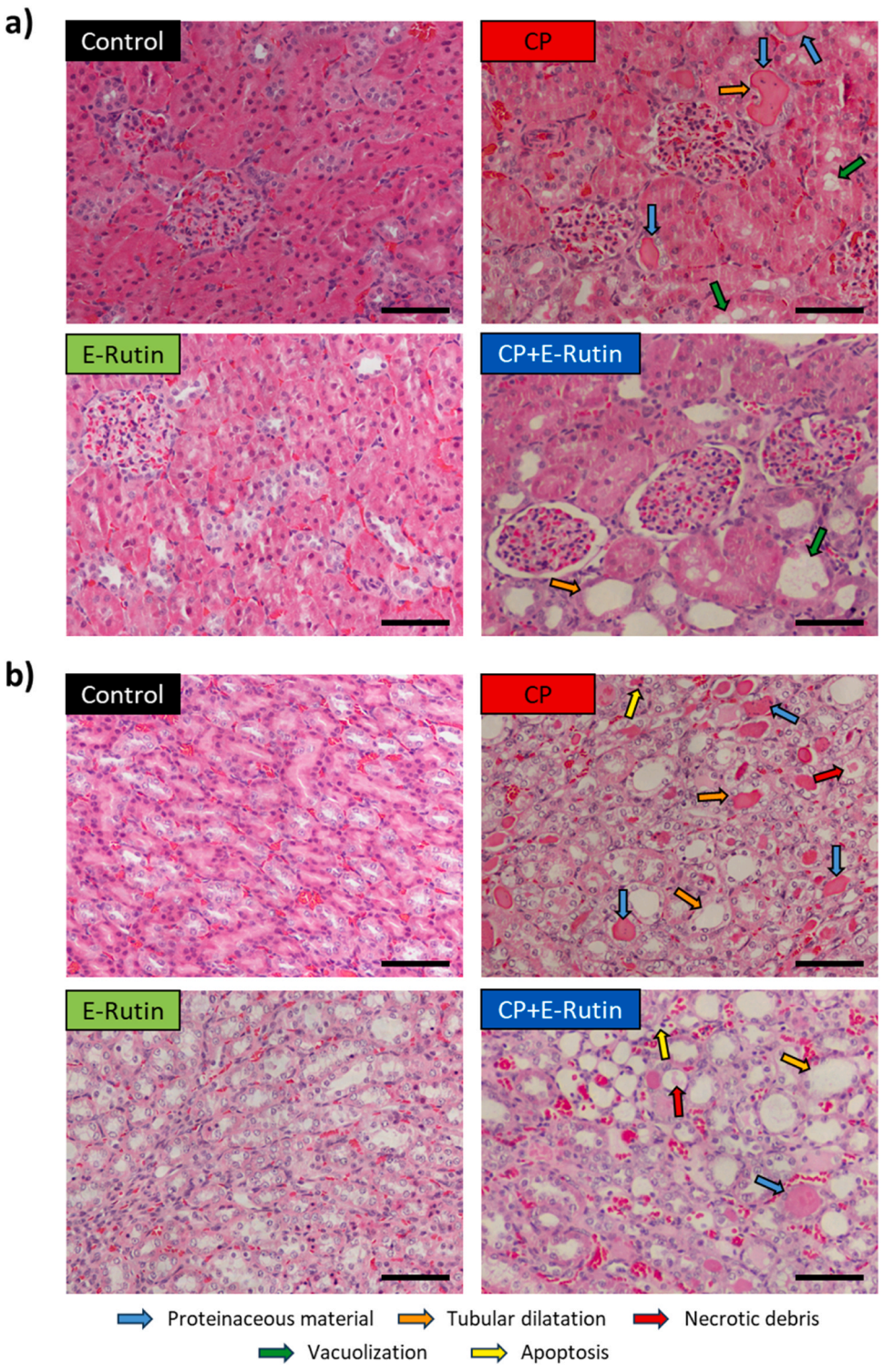

Fig. 12. Representative images of the renal cortex (a) and medulla (b) on day 12 of the experiment (scale bar: 100 μm). CP, cisplatin.

Whereas pure SAS-processed rutin showed faster dissolution rates and higher solubilities in simulated intestinal fluid compared to unprocessed rutin, the coating with Eudragit ® polymers provided a controlled solubilization profile. However, *in-vivo* experiments with these formulations failed to demonstrate a therapeutic effect against the nephrotoxicity caused by the cancer therapy drug cisplatin. Possible reasons for this negative result are a low *in-vivo* stability of the active compound, a poor bioabsorption or a damage induced by the cancer therapy drug that was too severe to be attenuated by the rutin formulation. Although E-Rutin did not show significant nephroprotective effects *in vivo*, the study provides valuable insights into the limitations of current polymeric encapsulation strategies for rutin. These findings highlight the importance of optimizing absorption and dosing, and future work should explore alternative formulations and test efficacy in models of milder nephrotoxicity.

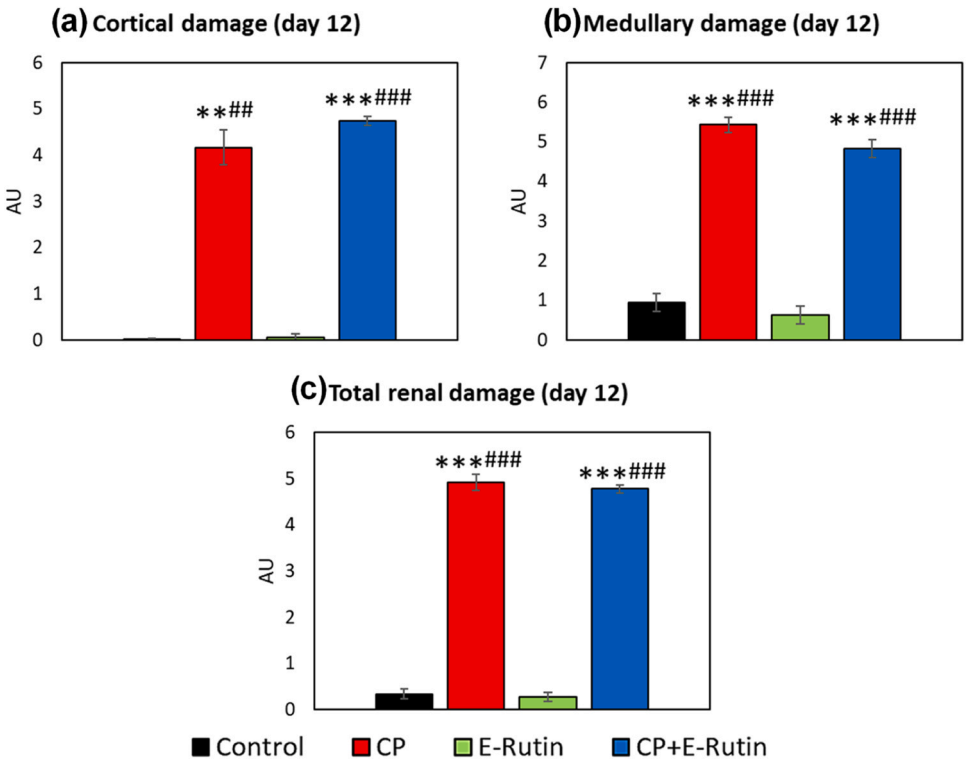

Fig. 13. Quantification of renal tissue damage, (a) Cortical damage, (b) Medullary damage and (c) Total renal damage, on day 12 of the experiment (n = 2 rats randomly selected x 5–15 images for groups Control, CP and E-Rutin; n = 4 rats x 5–15 images for group CP+E-Rutin). Data are presented as mean ± standard error of the mean. ** $p < 0.01$; *** $p < 0.001$ versus Control group; ## $p < 0.01$; ### $p < 0.001$ versus E-Rutin group. AU, arbitrary units; CP, cisplatin.

CRediT authorship contribution statement

Alfredo G. Casanova: Writing – original draft, Methodology, Investigation. **Ana I. Morales:** Writing – review & editing, Supervision, Funding acquisition, Conceptualization. **Martin Angel:** Writing – review & editing, Supervision, Funding acquisition, Conceptualization. **Marta Prieto:** Writing – review & editing, Methodology, Investigation, Conceptualization. **Iria Nerea Giraldes-Fernández:** Methodology, Investigation. **Sara Pahino-Villardón:** Methodology, Investigation. **Lucía Rodríguez-Lucas:** Methodology, Investigation.

Declaration of Competing Interest

The authors declare the following financial interests/personal relationships which may be considered as potential competing interests: Angel Martin reports financial support was provided by Government of Castile and León. Ana I. Morales reports financial support was provided by Carlos III Health Institute. Ana I. Morales reports financial support was provided by European Union. If there are other authors, they declare that they have no known competing financial interests or personal relationships that could have appeared to influence the work reported in this paper.

Acknowledgements

This project has been funded by Junta de Castilla y León (project "CLU-2019–04 – BIOECOUVA Unit of Excellence" of the University of Valladolid); and RICORS2040 (Kidney Disease) of the Instituto de Salud Carlos III (RD21/0005/0004 and RD24/0004/0024), co-funded by the European Union – NextGenerationEU, Mecanismo para la Recuperación y la Resiliencia (MRR).

Data availability

No data was used for the research described in the article.

References

[1] S. Samoni, S.D. Rosa, C. Ronco, G. Castellano, Update on persistent acute kidney injury in critical illnesses, Clin. Kidney J. 16 (2023) 1813, https://doi.org/10.1093/ckj/sfad107.
[2] X. Zhang, J. Wang, J. Zhang, Y. Tan, Y. Li, Z. Peng, Exosomes highlight future directions in the treatment of acute kidney injury, Int. J. Mol. Sci. 24 (2023) 15568, https://doi.org/10.3390/ijms242115568.
[3] I. Karimzadeh, E.F. Barreto, J.A. Kellum, L. Awdishu, P.T. Murray, M. Ostermann, A. Bihorac, R.L. Mehta, S.L. Goldstein, K.B. Kashani, et al., Moving toward a contemporary classification of drug-induced kidney disease, Crit. Care 27 (2023) 435, https://doi.org/10.1186/s13054-023-04720-2.
[4] K. Makris, L. Spanou, Acute kidney injury: definition, pathophysiology and clinical phenotypes, Clin. Biochem. Rev. 37 (2016) 85.
[5] T. Matsubara, H. Yokoi, H. Yamada, M. Yanagita, Nephrotoxicity associated with anticancer agents: perspective on onconephrology from nephrologists, Int J. Clin. Oncol. 28 (2023) 625–636, https://doi.org/10.1007/s10147-023-02307-z.
[6] S.S. Motwani, S.K. Sandhu, A. Kitchlu, Cisplatin nephrotoxicity: novel insights into mechanisms and preventative strategies, Semin. Nephrol. 42 (2022) 151341, https://doi.org/10.1016/j.semnephrol.2023.151341.
[7] S. Volovat, M. Apetrii, A. Stefan, C. Vlad, L. Voroneanu, M. Hogas, A. Haisan, C. Volovat, S. Hogas, Cisplatin and AKI: an ongoing battle with new perspectives—a narrative review, Int Urol. Nephrol. 55 (2023) 1205–1209, https://doi.org/10.1007/s11255-022-03418-8.
[8] N. Alassaf, H. Attia, Autophagy and necroptosis in cisplatin-induced acute kidney injury: recent advances regarding their role and therapeutic potential, Front. Pharmacol. 14 (2023), https://doi.org/10.3389/fphar.2023.1103062.
[9] A.G. Casanova, M. Harvat, L. Vicente-Vicente, Ó.J. Pellicer-Valero, A.I. Morales, F. J. López-Hernández, J.D. Martín-Guerrero, Regression modeling of the antioxidant-to-nephroprotective relation shows the pivotal role of oxidative stress in cisplatin nephrotoxicity, Antioxidants 10 (2021) 1355, https://doi.org/10.3390/antiox10091355.
[10] D. Zhang, G. Luo, K. Jin, X. Bao, L. Huang, J. Ke, The underlying mechanisms of cisplatin-induced nephrotoxicity and its therapeutic intervention using natural compounds, Naunyn-Schmiedes Arch. Pharmacol. 396 (2023) 2925–2941, https://doi.org/10.1007/s00210-023-02559-6.
[11] F. Ashrafi, Z. Ebrahimi, M. Nematbakhsh, Effect of short hydration on cisplatin-induced nephrotoxicity in cancer patients: a retrospective study, Int J. Hematol. Oncol. Stem Cell Res 11 (2017) 262–267.

[12] J. Li, Y. Wu, C. Chen, W. Zhang, L. Yue, T. Liu, A systematic review for prevention of cisplatin-induced nephrotoxicity using different hydration protocols and meta-analysis for magnesium hydrate supplementation, Clin. Exp. Nephrol. 28 (2024) 1–12, https://doi.org/10.1007/s10157-023-02386-2.
[13] S, H J, Y K, W Y, L Y, Z H, W X, L Y, L N-Acetylcysteine Attenuates Cisplatin-Induced Acute Kidney Injury by Inhibiting the C5a Receptor. BioMed research international (2019) https://doi.org/10.1155/2019/4805853.
[14] A. Rachman, S. Wafa, P. Nugroho, S. Koesnoe, The effect of mannitol addition to hydration on acute kidney injury event after high dose cisplatin chemotherapy: an ambispective cohort study, BMC Cancer 22 (2022) 395, https://doi.org/10.1186/s12885-022-09456-w.
[15] C. Xu, C. Lu, Z. Wang, X. Hu, S. Li, Y. Xie, Y. Qiu, R. Cao, Y. Li, J. Yang, Liraglutide abrogates nephrotoxic effects of chemotherapies, Pharmacol. Res. 189 (2023) 106680, https://doi.org/10.1016/j.phrs.2023.106680.
[16] A. Ullah, S. Munir, S.L. Badshah, N. Khan, L. Ghani, B.G. Poulson, A.-H. Emwas, M. Jaremko, Important flavonoids and their role as a therapeutic agent, Molecules 25 (2020), https://doi.org/10.3390/molecules25225243.
[17] C. Fang, D. Lou, L. Zhou, J. Wang, B. Yang, Q. He, J. Wang, Q. Weng, Natural products: potential treatments for cisplatin-induced nephrotoxicity, Acta Pharmacol. Sin. 42 (2021) 1951, https://doi.org/10.1038/s41401-021-00620-9.
[18] R.-Z. Tan, C. Wang, C. Deng, X. Zhong, Y. Yan, Y. Luo, H.-Y. Lan, T. He, L. Wang, Quercetin protects against cisplatin-induced acute kidney injury by inhibiting Mincle/Syk/NF-κB signaling maintained macrophage inflammation, Phytother. Res. 34 (2020) 139–152, https://doi.org/10.1002/ptr.6507.
[19] Z.U. Din, S.U. Farooq, M. Shahid, O. Alghamdi, N. Al-Hamoudi, F. Vohra, T. Abduljabbar, The Flavonoid 6-Hydroxyflavone Prevention of Cisplatin-Induced Nephrotoxicity, Histol. Histopathol. 35 (2020) 1197–1209, https://doi.org/10.14670/HH-18-251.
[20] C.L. Do Amaral, H.D.C. Francescato, T.M. Coimbra, R.S. Costa, J.D.C. Darin, L.M. G. Antunes, M.D.L.P. Bianchi, Resveratrol attenuates cisplatin-induced nephrotoxicity in rats, Arch. Toxicol. 82 (2008) 363–370, https://doi.org/10.1007/s00204-007-0262-x.
[21] B.D. Sahu, M. Kuncha, G.J. Sindhura, R. Sistla, Hesperidin attenuates cisplatin-induced acute renal injury by decreasing oxidative stress, inflammation and DNA damage, Phytomedicine 20 (2013) 453–460, https://doi.org/10.1016/j.phymed.2012.12.001.
[22] L.R. Fitzpatrick, T. Woldemariam, 5.16 - small-molecule drugs for the treatment of inflammatory bowel disease, in: S. Chackalamannil, D. Rotella, S.E. Ward (Eds.), Comprehensive Medicinal Chemistry III, Elsevier, Oxford, 2017, pp. 495–510. ISBN 978-0-12-803201-5.
[23] H. Hosseinzadeh, M. Nassiri-Asl, Review of the protective effects of rutin on the metabolic function as an important dietary flavonoid, J. Endocrinol. Invest 37 (2014) 783–788, https://doi.org/10.1007/s40618-014-0096-3.
[24] A. Ghorbani, Mechanisms of antidiabetic effects of flavonoid rutin, Biomed. Pharmacother. 96 (2017) 305–312, https://doi.org/10.1016/j.biopha.2017.10.001.
[25] A. Satari, S. Ghasemi, S. Habtemariam, S. Asgharian, Z. Lorigooini, Rutin: a flavonoid as an effective sensitizer for anticancer therapy; insights into multifaceted mechanisms and applicability for combination therapy, Evid. Based Complement Altern. Med. (2021) 9913179, https://doi.org/10.1155/2021/9913179.
[26] A. Ganeshpurkar, A.K. Saluja, The pharmacological potential of rutin, Saudi Pharm. J. 25 (2017) 149–164, https://doi.org/10.1016/j.jsps.2016.04.025.
[27] S. Biswas, M. Mondal, S. Pakhira, R. Ghosh, P. Samanta, J. Basu, A. Bhowmik, S. Hajra, P. Saha, Attenuation of paclitaxel-induced toxicities by polyphenolic natural compound rutin through inhibition of apoptosis and activation of NRF2/ARE signaling pathways, Food Chem. Toxicol. 200 (2025) 115408, https://doi.org/10.1016/j.fct.2025.115408.
[28] Y. Ma, P. Xu, H. Xing, Y. Zhang, T. Li, X. Ding, L. Liu, Q. Niu, Rutin mitigates fluoride-induced nephrotoxicity by inhibiting ROS-mediated lysosomal membrane permeabilization and the GSDME-HMGB1 axis involved in pyroptosis and inflammation, Ecotoxicol. Environ. Saf. 274 (2024) 116195, https://doi.org/10.1016/j.ecoenv.2024.116195.
[29] D. Muñoz-Reyes, A.I. Morales, M. Prieto, Transit and metabolic pathways of quercetin in tubular cells: involvement of its antioxidant properties in the kidney, Antioxid. (Basel) 10 (2021) 909, https://doi.org/10.3390/antiox10060909.
[30] A.R. Alhoshani, M.M. Hafez, S. Husain, A.M. Al-sheikh, M.R. Alotaibi, S.S. Al Rejaie, M.A. Alshammari, M.M. Almutairi, O.A. Al-Shabanah, Protective effect of rutin supplementation against cisplatin-induced nephrotoxicity in rats, BMC Nephrol. 18 (2017) 194, https://doi.org/10.1186/s12882-017-0601-y.
[31] W. Arjumand, A. Seth, S. Sultana, Rutin attenuates cisplatin induced renal inflammation and apoptosis by reducing NFκB, TNF-α and Caspase-3 expression in wistar rats, Food Chem. Toxicol. 49 (2011) 2013–2021, https://doi.org/10.1016/j.fct.2011.05.012.
[32] Y. Zhang, Q. Wang, Y.-D. Wang, B. Sun, X.-W. Leng, Q. Li, L.-Q. Ren, Effect of rutin on cisplatin-induced damage in human mesangial cells via apoptotic pathway, Hum. Exp. Toxicol. 38 (2019) 118–128, https://doi.org/10.1177/0960327118785233.
[33] R. Negahdari, S. Bohlouli, S. Sharifi, S. Maleki Dizaj, Y. Rahbar Saadat, K. Khezri, S. Jafari, E. Ahmadian, N. Gorbani Jahandizi, S. Raeesi, Therapeutic benefits of rutin and its nanoformulations, Phytother. Res. 35 (2021) 1719–1738, https://doi.org/10.1002/ptr.6904.
[34] Z. Ou-yang, X. Cao, Y. Wei, W.-W.-Q. Zhang, M. Zhao, J. Duan, Pharmacokinetic study of rutin and quercetin in rats after oral administration of total flavones of mulberry leaf extract, Rev. Bras. De. Farmacogn. 23 (2013) 776–782, https://doi.org/10.1590/S0102-695X2013000500009.
[35] E.U. Graefe, J. Wittig, S. Mueller, A.K. Riethling, B. Uehleke, B. Drewelow, H. Pforte, G. Jacobasch, H. Derendorf, M. Veit, Pharmacokinetics and bioavailability of quercetin glycosides in humans, J. Clin. Pharm. 41 (2001) 492–499, https://doi.org/10.1177/00912700122010366.
[36] A.M. Mohsen, M.A. Wagdi, A. Salama, Rutin loaded bilosomes for enhancing the oral activity and nephroprotective effects of rutin in potassium dichromate induced acute nephrotoxicity in rats, Sci. Rep. 14 (2024) 23799, https://doi.org/10.1038/s41598-024-73567-6.
[37] S.R. Croy, G.S. Kwon, Polymeric micelles for drug delivery, Curr. Pharm. Des. 12 (2006) 4669–4684, https://doi.org/10.2174/138161206779026245.
[38] H. Wu, M. Su, H. Jin, X. Li, P. Wang, J. Chen, J. Chen, Rutin-LOaded Silver Nanoparticles with Antithrombotic Function, Front Bioeng. Biotechnol. 8 (2020) 598977, https://doi.org/10.3389/fbioe.2020.598977.
[39] V. Surendran, N.N. Palei, Formulation and characterization of rutin loaded chitosan-alginate nanoparticles: antidiabetic and cytotoxicity studies, Curr. Drug Deliv. 19 (2022) 379–394, https://doi.org/10.2174/1567201818666211005090656.
[40] F.A. Alidoust, B. Rasti, H. Zamani, M. Mirpour, A. Mirzaie, Rutin-coated zinc oxide nanoparticles: a promising antivirulence formulation against pathogenic bacteria, World J. Microbiol Biotechnol. 40 (2024) 184, https://doi.org/10.1007/s11274-024-03984-2.
[41] C. Serri, V. Quagliariello, I. Cruz-Maya, V. Guarino, N. Maurea, P. Giunchedi, G. Rassu, E. Gavini, Hyaluronic acid-based nanoparticles loaded with rutin as vasculo-protective tools against anthracycline-induced endothelial damages, Pharmaceutics 16 (2024) 985, https://doi.org/10.3390/pharmaceutics16080985.
[42] Ch.N. Patra, R. Priya, S. Swain, G. Kumar Jena, K.C. Panigrahi, D. Ghose, Pharmaceutical significance of eudragit: a review, Future J. Pharm. Sci. 3 (2017) 33–45, https://doi.org/10.1016/j.fjps.2017.02.001.
[43] N. Wathoni, A.N. Nguyen, A. Rusdin, A.K. Umar, A.F.A. Mohammed, K. Motoyama, I.M. Joni, M. Muchtaridi, Enteric-coated strategies in colorectal cancer nanoparticle drug delivery system, Drug Des. Devel Ther. 14 (2020) 4387–4405, https://doi.org/10.2147/DDDT.S273612.
[44] B. Gullón, T.A. Lú-Chau, M.T. Moreira, J.M. Lema, G. Eibes, Rutin: a review on extraction, identification and purification methods, biological activities and approaches to enhance its bioavailability, Trends Food Sci. Technol. 67 (2017) 220–235, https://doi.org/10.1016/j.tifs.2017.07.008.
[45] W. Wang, M. Li, Y. Liu, B. Weigmann, Quercetin-loaded nanoparticles: a promising therapeutic strategy for inflammatory bowel disease, J. Inflamm. Res. 18 (2025) 12447–12461, https://doi.org/10.2147/JIR.S545203.
[46] M.J. Cocero, A. Martin, F. Mattea, S. Varona, Encapsulation and co-precipitation processes with supercritical fluids: fundamentals and applications, J. Supercrit. Fluids 47 (2009) 546–555, https://doi.org/10.1016/j.supflu.2008.08.015.
[47] F. Paola, I. de Marco, Eudragit: a novel carrier for controlled drug delivery in supercritical antisolvent coprecipitation, Polymers 12 (2020) 234, https://doi.org/10.3390/polym12010234.
[48] A. Arango-Ruiz, A. Martin, M.J. Cocero, C. Jiménez, J. Londoño, Encapsulation of curcumin using supercritical antisolvent (SAS) technology to improve its stability and solubility in water, Food Chem. 258 (2018) 256, https://doi.org/10.1016/j.foodchem.2018.02.088.
[49] G. Ozkan, S. Ilayda, S. Mottola, I. de Marco, E. Capanoglu, Supercritical antisolvent processing of propolis extract: solubility and release behaviour of bioactive compounds in different food simulants, Food Chem. 489 (2025) 144742, https://doi.org/10.1016/j.foodchem.2025.144742.
[50] A. Montes, L. Wehner, C. Pereyra, E.J. Martínez de la Ossa, Precipitation of submicron particles of rutin using supercritical antisolvent process, J. Supercrit. Fluids 118 (2016) 1–10, https://doi.org/10.1016/j.supflu.2016.07.020.
[51] A.G. Casanova, M. Prieto, C.I. Colino, C. Gutiérrez-Millán, B. Ruszkowska-Ciastek, E. de Paz, Á. Martín, A.I. Morales, F.J. López-Hernández, A micellar formulation of quercetin prevents cisplatin nephrotoxicity, IJMS 22 (2021) 729, https://doi.org/10.3390/ijms22020729.
[52] M. Fraile, R. Buratto, B. Gómez, Á. Martín, M.J. Cocero, Enhanced delivery of quercetin by encapsulation in poloxamers by supercritical antisolvent process, Ind. Eng. Chem. Res. 53 (2014) 4318–4327, https://doi.org/10.1021/ie5001136.
[53] R.T. Buratto, M.I. Chinchilla, M.J. Cocero, Á. Martín, Formulation of açaí (*E. Oleracea Mart.*) pulp and seeds extracts by co-precipitation in supercritical antisolvent (SAS) technology, J. Supercrit. Fluids 169 (2021) 105090, https://doi.org/10.1016/j.supflu.2020.105090.
[54] A. Martín, M.J. Cocero, Micronization processes with supercritical fluids: fundamentals and mechanisms, Adv. Drug Deliv. Rev. 60 (2008) 339–350, https://doi.org/10.1016/j.addr.2007.06.019.
[55] M.O. Iqbal, M.M. Ahmed, S. Arshad, U. Javaid, I.A. Khan, M. Manzoor, S. Andleeb, R. Riaz, S.H. Munawar, Z. Manzoor, et al., Nephroprotective effects of alhagi camelorum against cisplatin-induced nephrotoxicity in albino wistar rats, Molecules 27 (2022) 941, https://doi.org/10.3390/molecules27030941.
[56] R. Wang, W. Hassan, F. ud D. Ahmad, Q. Jabeen, H. Ahmed, O. Iqbal, Citrus aurantium ameliorates cisplatin-induced nephrotoxicity, BioMed. Res. Int. (2019) 3960908, https://doi.org/10.1155/2019/3960908.
[57] M.O. Iqbal, A.S. Sial, I. Akhtar, M. Naeem, A. Hazafa, R.A. Ansari, S.A.A. Rizvi, The nephroprotective effects of Daucus carota and eclipta prostrata against cisplatin-induced nephrotoxicity in rats, Bioengineered 12 (2021) 12702–12721, https://doi.org/10.1080/21655979.2021.2009977.
[58] K.M. Kamel, O.M. Abd El-Raouf, S.A. Metwally, H.A. Abd El-Latif, M.E. El-sayed, Hesperidin and rutin, antioxidant citrus flavonoids, attenuate cisplatin-induced nephrotoxicity in rats, J. Biochem Mol. Toxicol. 28 (2014) 312–319, https://doi.org/10.1002/jbt.21567.

[59] R.R. Radwan, S.M. Abdel Fattah, Mechanisms involved in the possible nephroprotective effect of rutin and low dose γ irradiation against cisplatin-induced nephropathy in rats, J. Photochem. Photobiol. B Biol. 169 (2017) 56–62, https://doi.org/10.1016/j.jphotobiol.2017.02.022.
[60] W.A. Ali, W.A. Moselhy, M.A. Ibrahim, M.M. Amin, S. Kamel, E.B. Eldomany, Protective effect of rutin and β-cyclodextrin against hepatotoxicity and nephrotoxicity induced by lambda-cyhalothrin in wistar rats: biochemical, pathological indices and molecular analysis, Biomarkers 27 (2022) 625–636, https://doi.org/10.1080/1354750X.2022.2087003.
[61] H. Zhang, H. Yang, S. Du, J. Ren, G. Qiao, J. Ren, Rutin ameliorates calcium oxalate crystal-induced kidney injury through anti-oxidative stress and modulation of intestinal flora, Urolithiasis 53 (2025) 50, https://doi.org/10.1007/s00240-025-01726-z.
[62] F.M. Kandemir, M. Ileriturk, C. Gur, Rutin protects rat liver and kidney from sodium valproate-induce damage by attenuating oxidative stress, ER stress, inflammation, apoptosis and autophagy, Mol. Biol. Rep. 49 (2022) 6063–6074, https://doi.org/10.1007/s11033-022-07395-0.
[63] Jaffe, M. Ueber Den Niederschlag, Welchen Pikrinsäure in Normalem Harn Erzeugt Und Über Eine Neue Reaction Des Kreatinins. 10 (2009) 391–400, https://doi.org/10.1515/bchm1.1886.10.5.391.
[64] Ó.J. Pellicer-Valero, G.A. Massaro, A.G. Casanova, M. Paniagua-Sancho, I. Fuentes-Calvo, M. Harvat, J.D. Martín-Guerrero, C. Martínez-Salgado, F.J. López-Hernández, Neural network-based calculator for rat glomerular filtration rate, Biomedicines 10 (2022) 610, https://doi.org/10.3390/biomedicines10030610.
[65] M.M. Bradford, A rapid and sensitive method for the quantitation of microgram quantities of protein utilizing the principle of protein-dye binding, Anal. Biochem 72 (1976) 248–254, https://doi.org/10.1006/abio.1976.9999.
[66] M.K. Das, B. Kalita, Design and evaluation of phyto-phospholipid complexes (phytosomes) of rutin for transdermal application, J. Appl. Pharm. Sci. 4 (2014) 051–057, https://doi.org/10.7324/JAPS.2014.401010.
[67] M. Jiao, Z.L. Wu, Y. Liu, W. Liu, R. Li, Surfactant-assisted separation of ginkgo flavonoids from Ginkgo biloba leaves using leaching and foam fractionation, AsiaPac. J. Chem. Eng. 11 (2016) 664–672, https://doi.org/10.1002/apj.1992.
[68] P. Franco, I. De Marco, Formation of rutin–β-cyclodextrin inclusion complexes by supercritical antisolvent precipitation, Polymers 13 (2021) 246, https://doi.org/10.3390/polym13020246.
[69] K. Selvaraj, R. Chowdhury, C. Bhattacharjee, Isolation and structural elucidation of flavonoids from aquatic fern azolla microphylla and evaluation of free radical scavenging activity, Int J. Pharm. Pharm. Sci. 5 (3) (2013) 743–749.
[70] Pharma Excipients. Technical Report on Eudragit® E100 Available online: ⟨https://www.pharmaexcipients.com/news/eudragit-e-100/⟩ (accessed on 28 January 2026).
[71] R.V. Haware, P.D. Chaudhari, S.R. Parakh, A. Bauer-Brandl, Development of a melting tablet containing promethazine HCl against motion sickness, AAPS PharmSciTech 9 (2008) 1006–1015, https://doi.org/10.1208/s12249-008-9133-x.
[72] M. Sharma, V. Sharma, A.K. Panda, D.K. Majumdar, Enteric microsphere formulations of papain for oral delivery, Yakugaku Zasshi 131 (2011) 697–709, https://doi.org/10.1248/yakushi.131.697.
[73] T.-H. Wu, F.-L. Yen, L.-T. Lin, T.-R. Tsai, C.-C. Lin, T.-M. Cham, Preparation, physicochemical characterization, and antioxidant effects of quercetin nanoparticles, Int J. Pharm. 346 (2008) 160–168, https://doi.org/10.1016/j.ijpharm.2007.06.036.
[74] Z.L. Tyrrell, Y. Shen, M. Radosz, Near-critical fluid micellization for high and efficient drug loading: encapsulation of paclitaxel into PEG-b-PCL micelles, J. Phys. Chem. C. 115 (2011) 11951–11956, https://doi.org/10.1021/jp202335r.
[75] V. Linares, C.J. Yarce, J.D. Echeverri, E. Galeano, C.H. Salamanca, Relationship between degree of polymeric ionisation and hydrolytic degradation of eudragit® e polymers under extreme acid conditions, Polymers 11 (2019) 1010, https://doi.org/10.3390/polym11061010.
[76] R. Mathur, S. Khan, R. Tripathi, S. Amin, S.D. Choudhary, Developing and applying a single strategy for improved intestinal permeability of diverse and complex phytomolecules: nanoformulations of rutin, quercetin, thymoquinone provide proof-of-concept, Adv. Pharm. Bull. (2024) 1, https://doi.org/10.34172/apb.39294.
[77] M.H. Asfour, A.M. Mohsen, Formulation and evaluation of pH-sensitive rutin nanospheres against colon carcinoma using HCT-116 cell line, J. Adv. Res. 9 (2018) 17–26, https://doi.org/10.1016/j.jare.2017.10.003.
[78] D. Dupeyrón, M. Kawakami, J. Rieumont, J.C. Carvalho, Formulation and CHaracterization of Anthocyanins-loaded Nanoparticles, Curr. Drug Deliv. 14 (2017) 54–64, https://doi.org/10.2174/1567201813666160915102151.
[79] E.S. Attar, V.H. Chaudhari, C.G. Deokar, S. Dyawanapelly, P.V. Devarajan, Nano drug delivery strategies for an oral bioenhanced quercetin formulation, Eur. J. Drug Metab. Pharm. 48 (2023) 495–514, https://doi.org/10.1007/s13318-023-00843-7.
[80] M. Sechi, D.N. Syed, N. Pala, A. Mariani, S. Marceddu, A. Brunetti, H. Mukhtar, V. Sanna, Nanoencapsulation of dietary flavonoid fisetin: formulation and *in vitro* antioxidant and α-glucosidase inhibition activities, Mater. Sci. Eng. C. Mater. Biol. Appl. 68 (2016) 594–602, https://doi.org/10.1016/j.msec.2016.06.042.
[81] J.V. Bonventre, Diagnosis of acute kidney injury: from classic parameters to new biomarkers, Contrib. Nephrol. 156 (2007) 213–219, https://doi.org/10.1159/000102086.
[82] R.N. El-Naga, Y.F. Mahran, Indole-3-carbinol protects against cisplatin-induced acute nephrotoxicity: role of calcitonin gene-related peptide and insulin-like growth factor-1, Sci. Rep. 6 (2016) 29857, https://doi.org/10.1038/srep29857.
[83] P.D. Sanchez-Gonzalez, F.J. Lopez-Hernandez, F. Perez-Barriocanal, A.I. Morales, J.M. Lopez-Novoa, Quercetin reduces cisplatin nephrotoxicity in rats without compromising its anti-tumour activity, Nephrol. Dial. Transplant. 26 (2011) 3484–3495, https://doi.org/10.1093/ndt/gfr195.
[84] L. Zhou, L. Zhang, Y. Zhang, X. Yu, X. Sun, T. Zhu, X. Li, W. Liang, Y. Han, C. Qin, PINK1 deficiency ameliorates cisplatin-induced acute kidney injury in rats, Front. Physiol. 10 (2019), https://doi.org/10.3389/fphys.2019.01225.
[85] W. Andlauer, C. Stumpf, P. Fürst, Intestinal absorption of rutin in free and conjugated Forms1, Biochem. Pharmacol. 62 (2001) 369–374, https://doi.org/10.1016/S0006-2952(01)00638-4.
[86] M. Carbonaro, G. Grant, Absorption of quercetin and rutin in rat small intestine, Ann. Nutr. Metab. 49 (2005) 178–182, https://doi.org/10.1159/000086882.
[87] A. Martín-Illana, R. Cazorla-Luna, F. Notario-Pérez, J. Rubio, R. Ruiz-Caro, A. Tamayo, M.D. Veiga, Eudragit® L100/chitosan composite thin bilayer films for intravaginal ph-responsive release of tenofovir, Int J. Pharm. 616 (2022) 121554, https://doi.org/10.1016/j.ijpharm.2022.121554.
[88] Y.B.G. Patriota, I.E.S. Arruda, A.C. de Jesus Oliveira, T.C. de Oliveira, E. de Lemos Vasconcelos Silva, L.L. Chaves, F. de Oliveira Silva Ribeiro, D.A. da Silva, M.F. de La Roca Soares, J.L. Soares-Sobrinho, Synthesis of eudragit® L100-coated chitosan-based nanoparticles for oral enoxaparin delivery, Int J. Biol. Macromol. 193 (2021) 450–456, https://doi.org/10.1016/j.ijbiomac.2021.10.111.
[89] B. Xu, W. Zhang, Y. Chen, Y. Xu, B. Wang, L. Zong, Eudragit® L100-coated mannosylated chitosan nanoparticles for oral protein vaccine delivery, Int J. Biol. Macromol. 113 (2018) 534–542, https://doi.org/10.1016/j.ijbiomac.2018.02.016.
[90] N.O. Al-Harbi, F. Imam, M.M. Al-Harbi, O.A. Al-Shabanah, M.R. Alotaibi, H.M. As Sobeai, M. Afzal, I. Kazmi, A.C. Al Rikabi, Rutin inhibits carfilzomib-induced oxidative stress and inflammation via the NOS-mediated NF-κB signaling pathway, Inflammopharmacology 27 (2019) 817–827, https://doi.org/10.1007/s10787-018-0550-5.
[91] I. Turan, D. Canbolat, S. Demir, G. Kerimoglu, F. Colak, N. Turkmen Alemdar, A. Mentese, Y. Aliyazicioglu, The ameliorative effect of primula vulgaris on cisplatin-induced nephrotoxicity in rats and quantification of its phenolic components using LC-ESI-MS/MS, Saudi Pharm. J. 31 (2023) 101730, https://doi.org/10.1016/j.jsps.2023.101730.
[92] K.A. Wargo, J.D. Edwards, Aminoglycoside-induced nephrotoxicity, J. Pharm. Pract. 27 (2014) 573–577, https://doi.org/10.1177/0897190014546836.